PNAS

Supporting Information for

Targeted demethylation and activation of *NLRC5* augment cancer immunogenicity through MHC class I

Xin Sun[1], Toshiyuki Watanabe[1], Yoshitaka Oda[2], Weidong Shen[3], Alaa Ahmad[1], Ryota Ouda[1], Paul de Figueiredo[4,5,6,7], Hidemitsu Kitamura[3,8], Shinya Tanaka[2,9], Koichi S. Kobayashi[1,4,10] *

Koichi S. Kobayashi
Email: kskobayashi@med.hokudai.ac.jp, kobayashi@tamu.edu

This PDF file includes:

Supplementary Material and Methods
Figures S1 to S11
Tables S1
Supplementary reference

Other supporting materials for this manuscript include the following:

Datasets S1 to S2

Mice
C57BL/6JJcl (B6; RRID:MGI:3055581) and BALB/cAJcl-*Foxn1*^{nu} (NUDE; RRID:MGI:3806503) mice were purchased from CLEA Japan, Inc. (Tokyo, Japan). C57BL/6-Tg (TcraTcrb) 1100Mjb/J (OT-I; RRID:IMSR_JAX:003831) mice were purchased from The Jackson Laboratory (Bar Harbor, ME, USA). Mice were bred and maintained in the Institution for Animal Experimentation at Hokkaido University Graduate School of Medicine in specific pathogen-free (SPF) conditions. Male and female mice at the age of 7–10 weeks-old were used in the subsequent experiments. All animal experiments were conducted according to the guidelines of the Hokkaido University Animal Experiment Implementation Manual and were approved by the Institutional Animal Care and Use Committee of Hokkaido University Graduate School of Medicine (Approval No. 19-0134, No. 23-0142).

Cell lines
Mouse melanoma B16F10 and human breast adenocarcinoma MCF7 cell lines were from RIKEN Bio BRC, Japan (Tsukuba, Japan, cat. RCB2630, RRID:CVCL_0159; cat. RCB1904, RRID:CVCL_0031). Human Lenti-X 293T cell line was from Takara Bio (Kasatsu, Japan. cat. 632180, RRID:CVCL_4401). MCF7, Lenti-X 293T, and B16F10 cell lines were cultured in Dulbecco's Modified Eagle Medium (DMEM, Nacalai, Kyoto, Japan, cat. 08458-16). For OT-I CD8+ T cell primary culture, cells were kept in Roswell Park Memorial Institute (RPMI) 1640 (Nacalai, cat. 30264-56) medium supplied with 50 μM of 2-mercaptoethanol (Life Technologies, Carlsbad, CA, cat. 21985023) and 2 mM of L-Glutamine (Life Technologies, cat. 25030081). All cell culture mediums were supplemented with 10% heat-inactivated fetal bovine serum (FBS; Nichirei, Kyoto, Japan, cat. 175012) and kept in 37 °C with 5% CO_2 in a humidified incubator. All the cell lines were tested negative for mycoplasma contamination.

Plasmids
Lenti dCAS-VP64 Blast (Addgene, Watertown, NY, USA, cat. #61425), lenti MS2-P65-HSF1 Hygro (Addgene, cat. #61426) and lenti sgRNA (MS2) zeo backbone (Addgene, cat. #61427) were gifts from Feng Zhang. To accommodate insertion of *TET1cd*, additional restriction sites, *Xba*I and *BstB*I, were inserted between *BamH*I and *BsrG*I in Lenti dCAS-VP64 Blast and lenti MS2-P65-HSF1 Hygro by restriction digestion and ligation cloning. Human *TET1cd* was amplified by PCR from pPlatTet-grna2 (Addgene, cat. #82559, a gift from Izuho Hatada) with either *BamH*I-*Xba*I or *BamH*I-*BstB*I as restriction sites and ligated into lenti dCAS-VP64 Blast and lenti MS2-P65-HSF1 Hygro. As a result, lenti dCAS9-TET1CD, lenti MS2-TET1CD (using *BamH*I, *Xba*I, flanking VP64 in lenti dCAS-VP64 Blast and P65-HSF1 in lenti MS2-P65-HSF1 Hygro) and lenti dCAS9-TET1CD-VP64, lenti MS2-TET1CD-P65-HSF1 (using *BamH*I, *BstB*I) were generated. For cloning of sgRNA, oligonucleotides encoding sgRNA target sites were custom ordered (Life Technologies), phosphorylated by T4 polynucleotide kinase (NEB, Ipswich, MA, USA, cat. M0201), denatured, annealed, and inserted into *BsmB*I by golden gate assembly of lenti sgRNA (MS2) zeo (Addgene, cat. #61427, a gift from Feng Zhang) as described previously (1). Unmodified lenti sgRNA (MS2) zeo was used to express scrambled control sgRNA.

Generation of stable cell lines
All the lentiviral vectors were generated using Lenti-X 293T cell line. Specifically, 5×10^5 Lenti-X 293T cells were seeded in 6-well plate and incubated overnight. Total 3 μg of target lentiviral plasmids, pCMV-VSV-G and psPAX2 plasmids (Addgene, #8454 a gift from Bob Weinberg; cat. #12260, a gift from Didier Trono) were at 1ug:1ug:1ug ratio, subsequently, the plasmids mixture was incubated with 15 μg of Polyethylenimine max (1μg μl^{-1}; PEI MAX, Polysciences, Warrington, PA, USA, cat. 24765-1) for 15 min. DNA-PEI mixture was added dropwise into 6-well plate and incubated for 6 h before the culture medium was replaced with refresh medium and cells were incubated for additional 42 h. The lentiviral vector containing media was centrifuged at 500× g for 3 min to remove cells and debris and supernatant was filtered through 0.45 μM filter (Sartorius stedim, Göttingen, Germany, cat. S7598-FXOSK). Next, 1.5 ml of lentiviral vector containing media was added to the target cells in 6-well plate with 8 μg ml^{-1} of polybrene (Nacalai Tesque, cat. 12996-

81) and incubated for 48 h. Subsequently, stably transduced cells were selected by corresponding antibiotics.
For B16F10, cells were co-transduced by lenti dCAS9-TET1CD and lenti MS2-TET1CD (B16F10-TD-I) or lenti dCAS9-TET1CD-VP64 and lenti MS2-TET1CD-P65-HSF1 (B16F10-TRED-I). Subsequently, stably transduced cells were co-selected by 1.25 μg ml^{-1} of blasticidin (KAKEN PHARMACEUTICAL, Tokyo, Japan, cat. KK-400) and 125 μg ml^{-1} of hygromycin (InvivoGen, San Diego, CA, USA, cat. ant-hg-1) for 6 d. For B16F10-TD-I, single cell clones were generated before sgRNA transduction. Subsequently, lenti sgRNA (MS2) zeo expressing various sgRNAs were transduced into B16F10-TD-I and B16F10-TRED-I and stably transduced cells were selected by 120 μg ml^{-1} of zeocin (Life Technologies, cat. R25001) for 10 d.
For MCF7, cells were sequentially transduced with lenti dCAS9-TET1CD-VP64, lenti MS2-TET1CD-P65-HSF1, and lenti sgRNA (MS2) zeo to generate MCF7-TRED-I cells. After each transduction, stably transduced cells were sequentially selected by 25 μg ml^{-1} of blasticidin, 250 μg ml^{-1} of hygromycin for 7 d, and 500 μg ml^{-1} of zeocin for 10 d, respectively.
Successful integration of lentiviral vector construct was confirmed by qRT-PCR quantification of lentiviral transfer vector gene expression and resistance to corresponding antibiotics. Antibiotics were removed from culture medium after confirmation of successful integration.

Quantitative reverse transcription PCR (qRT-PCR)
To quantify mRNA expression levels, approximate 1×10^5 B16F10-TD-I, B16F10-TRED-I, or 1.5×10^5 MCF7-TRED-I cells were seeded in 12 well plate on day 0. From day 1, cells were stimulated with 20 ng ml^{-1} of mouse interferon-γ (mIFN-γ) (BioLegend, San Diego, CA, USA, cat. 575302) or left unstimulated for 24 h. Subsequently, cells were homogenized in Sepasol (Nacalai, cat. 09379-55) and total RNA was extracted according to manufacturer's instructions. RNA was reverse transcribed into cDNA using ReverTra Ace qPCR RT Master Mix (Toyobo, Osaka, Japan, cat. FSQ-301), and qRT-PCR was performed using THUNDERBIRDTM SYBR qPCR Mix reagent (Toyobo, cat. QPS-201) in StepOne qRT-PCR instrument (Life Technologies). Mouse or human *Nlrc5/NLRC5, H2-K^b, H2-D^b, HLA-A, HLA-B, HLA-C, Lmp2/LMP2, Tap1/TAP1, B2m/B2M, Ciita/CIITA, Mx1/MX1* and *Gapdh/GAPDH* were amplified by specific primers. *Gapdh/GAPDH* was used to normalize the value and relative gene expression level was calculated as fold change compared with the control samples using 2^(ΔΔCt) method. The sequence information of primers used in qRT-PCR is listed in Table S1.

Flow cytometry
To evaluate surface MHC class I expression levels *in vitro*, 5×10^4 B16F10-TD-I, B16F10-TRED-I or 1×10^5 MCF7-TRED-I cells were seeded in 12-well plates and incubated for 48 h with or without 20 ng ml^{-1} of mIFN-γ stimulation. Subsequently, cells were detached by trypsinization and resuspended in FACS buffer (2% FBS in PBS). Next, cells were stained by FITC H2-K^b/D^b (BioLegend, cat. 114605, RRID:AB_313596), or FITC H2-K^b (BioLegend, cat. 116505, RRID:AB_313733), or PE-H2-D^b/D^d (BioLegend, cat. 114507, RRID:AB_313588) antibodies and MCF7 was stained by PE HLA-A,B,C (BioLegend, cat. 311405, RRID:AB_314874) or PE HLA-A2 (BioLegend, cat. 343305, RRID:AB_1877228) or AF647 HLA-B (BD, Franklin Lakes, NJ, USA, cat. 569663) for 30 min on ice. Stained cells were washed twice and resuspended in FACS buffer and acquired by FACSCanto II.
To characterize tumor-infiltrating lymphocytes (TILs) and cancer cells *in vivo*, tumors were fragmented by scissors and filtered through a 70 μm cell strainer (AS ONE, Osaka, Japan, cat. VCS-70) to generate single cell suspension. Red blood cells were lysed for 5 min on ice in 1 ml ammonium-chloride-potassium (ACK) lysis buffer (Life Technologies, cat. A1049201).
To distinguish alive cells, 3×10^6 dissociated tumor cells were stained by 100 μl Zombie Violet Fixable Viability dye (1:1000 dilution in PBS; BioLegend, cat. 423113) at 25 °C for 15 min. Subsequently, tumor cells were aliquoted into two tubes for characterization of TILs (2×10^6) or tumor cells (1×10^6).
To characterize TILs, Zombie dye-stained cells were further stained with the following antibodies (all from BioLegend, 1:100 dilution): APC-Cy7 CD45.2 (cat. 109824, RRID:AB_830789), FITC CD4 (cat. 100405, RRID:AB_312690), APC CD8a (cat. 100712, RRID:AB_312751), PE IFN-γ (cat. 505808, RRID:AB_315402), and PerCP-cy5.5 CD44 (cat. 103032, RRID:AB_2076204). Cells were

incubated with antibodies for surface markers in 100 µl FACS buffer on ice for 30 min. Subsequently, cells were fixed by incubating with 4% PFA for 15 min on ice, and then permeabilized with 1× intracellular staining permeabilization wash buffer (BioLegend, cat. 420801) according to manufacturer's instructions. Subsequently, cells were incubated with PE IFN-γ antibody in 100 µl 1× intracellular staining buffer for 30 min on ice.
To quantify MHC class I and PD-L1 levels in tumor cells *in vivo*, 1×10^6 Zombie dye-stained cells were further stained with APC-Cy7 CD45.2, FITC H-2K^b/D^b, and PE PD-L1 (cat. 124308, RRID:AB_2073556), in the same manner as TILs surface marker staining.
Samples were acquired using an BD FACS Canto II flow cytometer. Specific antibody binding was ensured by staining with corresponding isotype antibodies. Collected data were analyzed using FlowJo v10.6.2. (BD).

Assessment of DNA methylation level
Cells were digested by proteinase K (Fujifilm Wako Pure Chemical Corp, Osaka, Japan, cat.161-28701) overnight, subsequently, genomic DNA was extracted by ethanol precipitation and residual RNA was removed by incubating with RNase A (10 µg ml^{-1}, NIPPON GENE, Tokyo, Japan, cat. 313-01461) for 30 min at 37 °C. Bisulfite conversion and purification were performed using 500 ng of genomic DNA with EZ DNA Methylation Kit (Zymo Research, Irvine, CA, USA, cat. D5001) according to manufacturer's instructions. Fragment of human and mouse NLRC5 promotor region in the converted genomic DNA was amplified by PCR using AmpliTaq Gold 360 Master Mix (Life Technologies, cat. 4398876) and specific primers. PCR products were either sequenced directly or cloned into pBlueScript II SK(+) by SLiCE method (2) before sanger sequencing. For direct sanger sequencing of PCR product, percentage of methylated cytosine was calculated by (fluorescence intensity of guanine)/(fluorescence intensity of guanine + thymine) in the cytosine of CpG dinucleotides.

Chromatin immune precipitation-quantitative PCR (ChIP-qPCR)
Approximately 10^6 of B16F10 TD-I and TRED-I sgScramble and sg*Nlrc5* cells were cross-linked with 1% formaldehyde for 10 min and stopped by 0.125 M glycine for 10 min. Cells were lysed in SDS lysis buffer and were sonicated to generate shared DNA (20 times of 30s on-off cycles; Picoruptor, Diagenode, Denville, NJ, US). Sonicated lysates were centrifuged and supernatant were incubated with anti-Histone H3 (acetyl K9 + K14 + K18 + K23 + K27) antibody (abcam, Cambridge, UK, cat. ab47915, RRID:AB_873860) or Normal Rabbit IgG (Cell Signaling, Danvers, MA, US, cat. 2729S, RRID:AB_1031062) at 1:100 dilution overnight. Following a 2-hour incubation with Pierce Protein A/G Agarose (Life Technologies, cat. 20422) at 1:20 dilution. Samples were washed sequentially by low salt buffer, high salt buffer, LiCl, and Tris-EDTA. Cross-links were reversed by 5 M NaCl at 65 °C for 4 h, followed by RNase A at 37 °C for 30 min and proteinase K at 55 °C for 1 h. DNA was purified by phenol-chloroform method and analyzed by qRT-PCR using primers enlisted in Table S1.

Isolation of OT-I CD8+ T cells from spleen
Spleen from 7-10 weeks old OT-I transgenic mice were dissociated by slide glass. Single cell suspension was generated by passing cells through 48 µm mesh (San-web, Tokyo, Japan, cat. 91-1189). Red blood cells (RBCs) were lysed by incubation in ACK lysing buffer for 5 min on ice. Subsequently, OT-I CD8+ T cells were isolated by positive selection using BD IMag system (BD, magnet: cat. 552311; CD8a Particles: cat. 551516) according to manufacturer's instruction and used for co-culture experiments.

OT-I T cell activation assay
B16F10-TD-I sgScramble and sg*Nlrc5* or B16F10-TRED-I sgScramble or sg*Nlrc5* cells were seeded at 3×10^4 or 6×10^4 cells per well in 48-well plate and loaded with 0, 1, and 2 or 0, 0.0625, 0.125, 0.25, 0.5, and 1 µg ml^{-1} of Ovalbumin (OVA) peptide (257-264) SIINFEKL (PEPTIDE INSTITUTE, Osaka, Japan, cat. POV-3659-PI) overnight. Unbound OVA peptides were washed away with PBS the next day. Isolated OT-I CD8+ T cells were added at 2×10^5 or 3×10^5 per well to each well and co-cultured with B16F10 cells for 24 h in total. Monensin (Life Technologies, cat. 00-4505-51) was treated to each well at concentration of 2 µM to accumulate intracellular cytokine for

6 h before harvest. Cells were resuspended in PBS and stained by 1:1000 Zombie violet viability dye (BioLegend, cat. 423113) for 15 min at room temperature followed by surface marker staining by APC CD8 and FITC CD69 (Life Technologies, cat. 11-0691-82, RRID:AB_465119) for 30 min on ice. Subsequently, cells were fixed by 4% paraformaldehyde phosphate buffer (PFA, Nacalai, cat. 09154-85) on ice for 15 min. Next, cells were permeabilized by 1x permeabilization buffer (BioLegend, cat. 421002) according to manufacturer's instruction. Finally, cells were stained by PE IFN-γ for 30 min in 1x permeabilization buffer on ice. After washing, samples were acquired by FACSCanto II.

OT-I T cell killing assay

B16F10-TRED-I sgScramble and sg*Nlrc5* cells were stained by 5 μM carboxyfluorescein diacetate succinimidyl ester (CFSE, Tonbo Biosciences, 13-0850-U500) for 10 min in the dark and seeded at 2.5×10^4 cells per well in 48-well plate. Cells were loaded with 0.5 μg ml^{-1} of OVA peptide overnight. Unbound OVA peptides were washed away with PBS. Purified OT-I CD8+ T cells were added to the media at OT-I:B16 ratio of 10:1, 5:1, 2.5:1, and 1.25:1 and co-cultured for additional 48 h. Cells were detached by trypsinization and stained by 1:1000 PBS diluted Zombie Violet for 15 min at room temperature. After washing, samples were acquired by FACSCanto II.

Whole tumor lysate vaccination

Approximate 1×10^6 B16F10 TRED-I cells were used for each mouse. Cells were lysed by liquid nitrogen-37 °C water bath freeze-thaw cycle for 5 times. The lysate was centrifuged and the supernatant was mixed with complete Freund's adjuvant (CFA, Sigma-Aldrich, St. Louis, MO, US, cat. F5881) by syringe to make antigen emulsion. Female 10-week-old C57BL/6 mice were intradermally injected with 100 μl of antigen emulsion in the flank on day 0. The immune response was boosted by the injection of lysate-IFA (Incomplete Freund's Adjuvant, Sigma-Aldrich, cat. F5506) emulsion on day 7. CD8+ T cells were isolated from splenocytes and co-cultured with 5×10^4 B16F10 TRED-I sgScramble or sgNlrc5 cells at 8:1 or 4:1 ratio for 24 h in total, with 6 h of 2 μM Monensin treatment before harvest. CD8+ T cells were isolated and stained similarly as OT-I T cell activation experiments.

Subcutaneous B16F10 melanoma model

To investigate the effect of targeted demethylation and activation of *Nlrc5* on tumor growth *in vivo*, female and male C57BL/6, NUDE or C57BL/6 mice depleted for CD8+ T cells by anti-CD8a antibody injection (i.p. injection at 400 μg per mouse on Day -1 and 3; ichorbio, Wantage, UK, cat. ICH1045, RRID:AB_2921447) were subcutaneously injected with 3×10^5, 5×10^5, or 5×10^5 of B16F10-TRED-I sgScramble and sg*Nlrc5* cells on Day 0 in 100uL PBS in the left flank using 26G needle and 1 ml syringe. Tumor volume was estimated daily or every other day by digital caliper after tumors were visually apparent and tumor volume was estimated by the following formula: Tumor Volume (mm^3) = length × width × width /2 (3). Mice were euthanized on day 18 for C57BL/6, day 15 for NUDE, or day 13 for CD8+ T cell-depleted C57BL/6, and tumors were harvested and used for flow cytometry, RNA-seq, and immunohistochemistry analysis.

To investigate the effect of targeted demethylation and activation of *Nlrc5* on efficacy of anti-PD-1 treatment *in vivo*, female and male C57BL/6 mice were implanted with 6×10^5 of B16F10-TRED-I sgScramble or sg*Nlrc5* cells on the single flank (unilateral model) or on the opposite flanks (bilateral model) similarly as described above. Subsequently, mice were randomly divided into isotype and PD-1 groups. Each group was intraperitoneally injected with 250 μg $100ul^{-1}$ of isotype control (leinco, Fenton, MO, USA, cat. I-1177, RRID:AB 2737530) or anti-PD-1 antibody (leinco, cat. P362, RRID:AB_2737557) every other day from day 3, for total of 5 times. Tumor volume was estimated every other day from day 3 similarly as described above. Mice were euthanized on day 15 in sgScramble and day 18 in sg*Nlrc5* group (unilateral model), or day 17 (bilateral model) and tumors were harvested for flow cytometry analysis.

Hematoxylin and eosin (H&E) staining and immunohistochemistry (IHC)

B16F10-TRED-I sgScramble and sg*Nlrc5* tumors were snap frozen by liquid nitrogen immediately after harvest and kept at −80 °C until IHC analysis. Tumors were fixed in 10% formalin, dehydrated with increasing concentrations of ethanol, and then impregnated with and embedded in paraffin.

Tissue blocks were sectioned and deparaffinized in xylene, washed in PBS (pH 7.4), and rehydrated in a graded series of ethanol solutions for hematoxylin and eosin (H&E) staining with a standard protocol. For IHC, heat-mediated antigen retrieval was performed in Tris/EDTA buffer (pH 9.0) at 97 °C for 20 min. The sections were treated with 0.3% hydrogen peroxidase for 5 min to quench endogenous peroxidase activity. After saturation with serum, primary antibody of anti-CD8 (1:300 dilution, 4 °C overnight incubations; Cell Signaling, Danvers, MA, USA, cat. 98941, RRID:AB_2756376) and anti-CD3 (1:75 dilution, 25 °C 60 min incubations; GeneTex, Irvine, CA, USA, cat. GTX16669, RRID:AB_425123) were used for staining. After washing in PBS, slides were incubated with biotinylated goat anti-rabbit immunoglobulin antibody for 30 min at room temperature. Visualization of antibody specific binding were performed with freshly prepared 3,3′-diaminobenzidine tetrahydrochloride. The intensity of the staining was analyzed by HistoQuest software (TissueGnostics, Vienna, Austria). Sites with representative staining were selected in the center and margin of tumors and staining intensity was calculated by ImageJ (4).

Analysis of methylation status of the NLRC5 promoter in human melanoma

DNA methylation profile of human nonmalignant skin tissue and breast tissue were accessed through Gene Expression Omnibus (GEO; Accession number: GSE51954, GSE88883) (5-7). DNA methylation and transcriptome profiles of melanoma tissue from the Cancer Genome Atlas skin cutaneous melanoma (TCGA SKCM) cohort and invasive breast cancer (TCGA BRCA) cohort were obtained from UCSC XENA (8-10). Immune cell infiltration estimation of TCGA SKCM and BRCA cohorts was from TIMER (11). We used the averaged β values of methylated CpG site (cg08159663, cg07839457, and cg16411857) in the *NLRC5* promoter to represent mean *NLRC5* methylation levels. The mean *NLRC5* methylation level was used in the correlation analysis with *NLRC5* expression and estimated immune cells infiltration levels.

RNA sequencing

Total RNA was extracted using Sepasol according to the manufacturer's instructions and assessed for RNA Integrity Number using Agilent 2100 Bioanalyzer (Agilent Technologies, Santa Clara, CA, USA). Poly(A)-tailed mRNA was selected with beads using the NEBNext Poly(A) mRNA Magnetic Isolation Module (NEB, cat. E7490). RNA-seq libraries were prepared using the NEBNext Ultra II Directional RNA Library Prep Kit (NEB, cat. E7760) according to the manufacturer's instructions. Sequencing of 150 nucleotide-long paired-end reads was performed on the NovaSeq 6000 (illumina).

The sequencing data were aligned to mouse genome (GRCm39/mm39) using STAR aligner (v2.7.10a) (12). Raw gene counts were obtained by STAR --quantMode GeneCounts option and loaded into R (v4.2.1) for data normalization and differential expression analysis by DESeq2 (v1.36) (13). Genes with adjusted $p < 0.05$ (Benjamini–Hochberg method) and |Fold change| > 2 were considered significantly differentially expressed. Gene ontology (GO) enrichment analysis was performed using clusterProfiler (14). The false discovery rate (FDR) < 0.001 and the normalized enrichment score |NES| > 2 was considered as significantly altered pathway.

Statistical analysis

For *in vivo* tumor growth analysis, significance was analyzed using 2-way ANOVA test. For others, significance was analyzed using either Fisher's LSD test or two-tailed unpaired Student's *t*-test. A *p*-value of less than 0.05 was regarded as statistically significant. Error bars represents mean values ±SEM in tumor growth curve and ±SD in others. All statistical analyses were performed using GraphPad Prism software (v9.3.1).

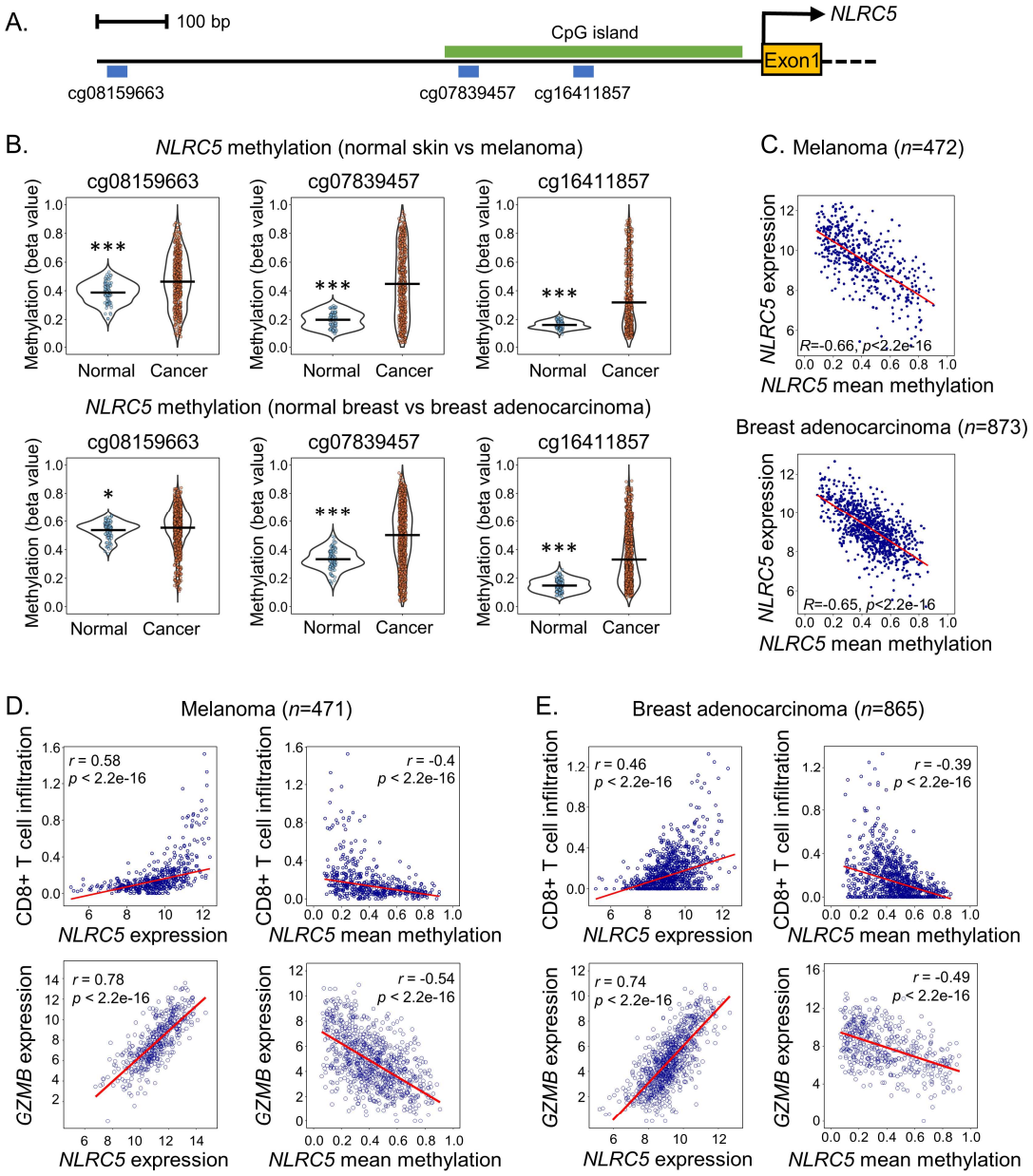

Fig. S1 Hypermethylation of the *NLRC5* promoter negatively correlates with *NLRC5* expression, immune cell infiltration and activation. (A) Schematic illustration of targeting sites of illumina 450k methylation probes in the *NLRC5* promotor with high methylation level in melanoma and breast invasive carcinoma. (B) The DNA methylation status of *NLRC5* promoter was compared between normal skin (*n* = 78) and melanoma tissues (SKCM) (*n* = 475), or normal breast (*n* = 100) and breast invasive carcinoma (BRCA) (*n* = 888) using representative CpG sites (cg08159663, cg16411857, and cg07839457) of the *NLRC5* promoter. (C) Scatter plot showing the correlation between mean methylation level of the *NLRC5* promoter (cg08159663, cg16411857, and cg07839457) and *NLRC5* expression levels in melanoma and breast invasive carcinoma tissue. (D,E) Scatter plot of the correlation of *NLRC5* expression or methylation levels with estimated CD8+ T cell infiltration scores or *GZMB* expression levels in (D) skin melanoma and (E) breast invasive carcinoma tissue. '*n*' stands for number of patients. Statistical significance was

determined by unpaired two-sided student's *t*-test in (B). * $p < 0.05$; *** $p < 0.001$. Pairwise correlations in (C,D,E) were calculated using the Pearson correlation test.

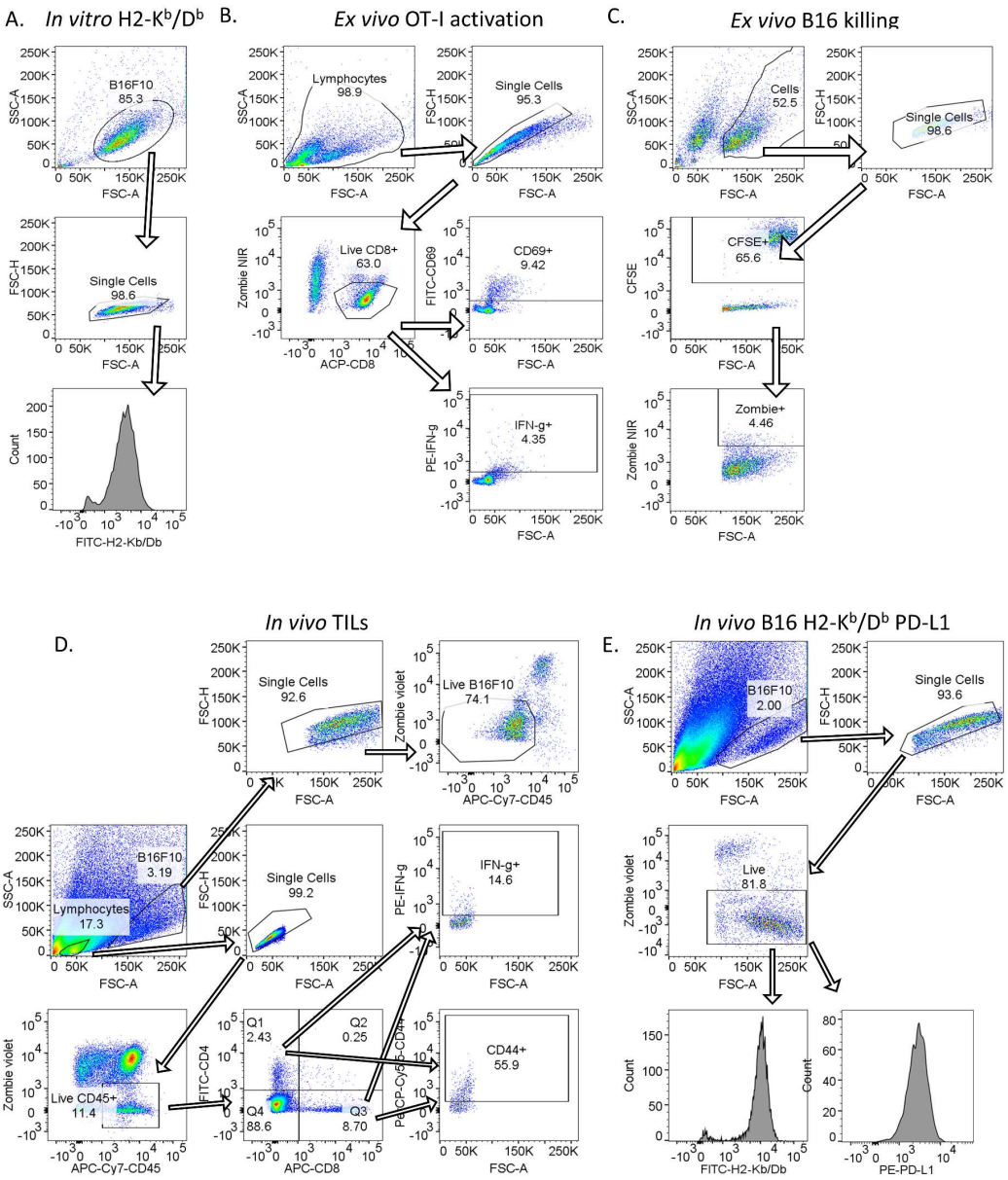

Fig. S2 Gating strategy for flow cytometry analysis. (A) Quantification of MHC class I levels on B16F10 and MCF7 cell lines *in vitro*. Corresponding to Fig. 1H, 2E, and 6F. Cultured cells were gated by size using FSC-A and SSC-A and singlets were gated by FSC-A and FSC-H. (B) Characterization of OT-I T cells activation status in co-culture *ex vivo*. Corresponding to Fig. 1I, 2F, Fig. S3A,B, and S6B,C. Live OT-I T cells were gated by FSC-A, SSC-A, FSC-H, Zombie NIR–, and CD8+. Activated OT-I T cells were gated as IFN-γ+ and CD69+. (C) Quantification of dead B16F10-TRED-I cells in co-culture with OT-I T cells *ex vivo*. Corresponding to Fig. 2G and Fig. S3C. CSFE labeled B16F10-TRED-I cells were gated as FITC+. Dead cells were gated as Zombie NIR+. (D) Characterization of tumor infiltrating lymphocytes and quantification of viable B16F10 cells *in vivo*. Corresponding to Fig. 3E, 5D, and Fig. S7, S10. Single live nucleated hematopoietic cells were gated based on FSC-A, SSC-A, SSC-H, Zombie NIR–, and CD45+ signals. Subsequently, CD4+ or CD8+ T cells were gated by CD4+ or CD8+, followed by gating IFN-γ+ and CD44+ cells to identify activated/memory lymphocytes. Single B16F10-TRED-I cells were determined by FSC-A, SSC-A, SSC-H, and viable B16F10-TRED-I cells were determined as Zombie NIR– and CD45–.

(E) Quantification of H2-K^b/D^b and PD-L1 levels on B16F10 cells *in vivo*. Corresponding to Fig. 3F and 5E. Single live B16F10 cells were gated by FSC-A, SSC-A, SSC-H, Zombie NIR–, and CD45–.

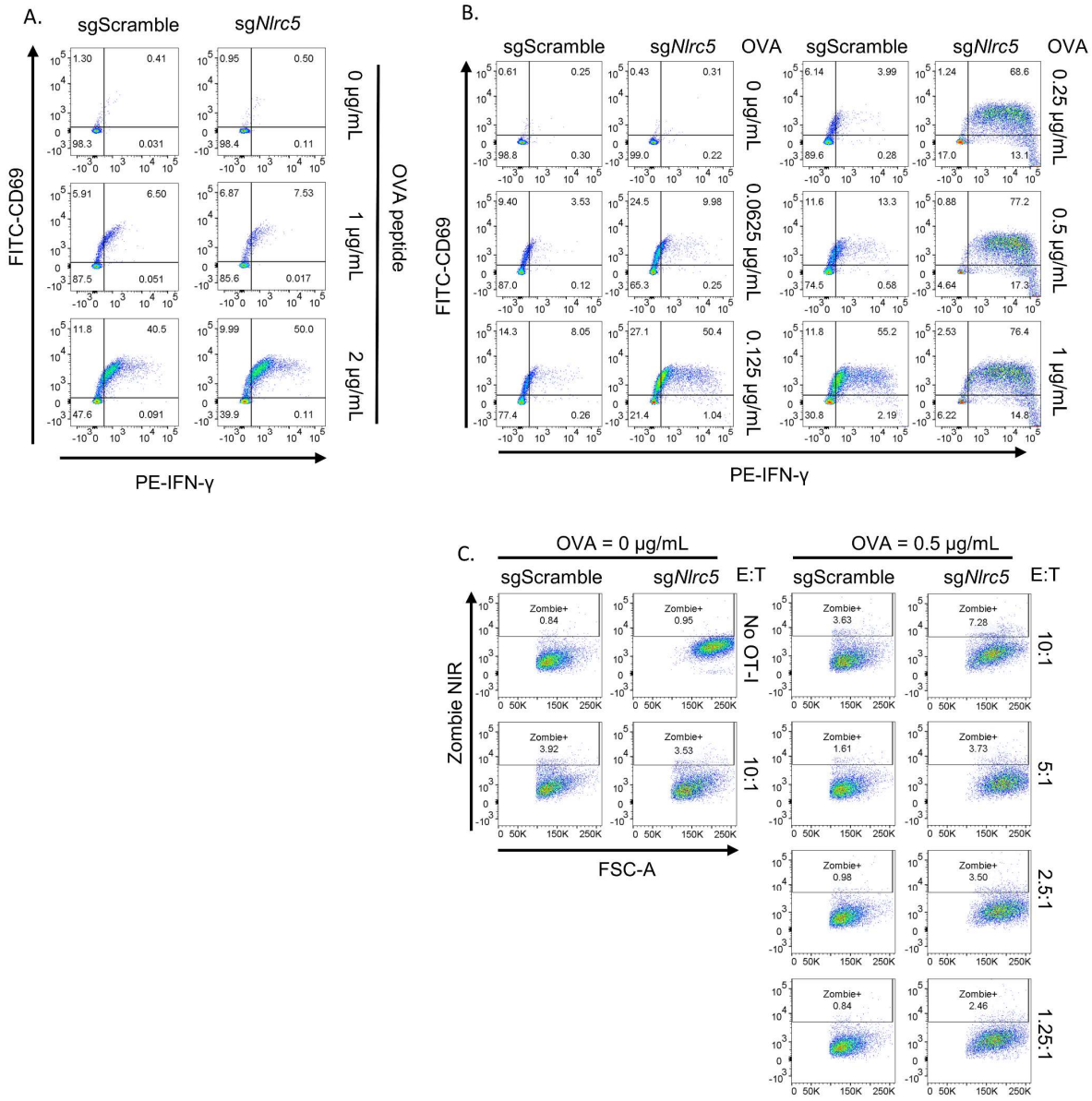

Fig. S3 Representative scatter plots by flow cytometry analysis in *ex vivo* co-culture experiments. OT-I CD8+ T cells were co-cultured with B16F10-TD-I and B16F10-TRED-I cells stably transduced with sgScramble or sg*Nlrc5*. IFN-γ and CD69 expression levels of OT-I T cells was evaluated by flow cytometry when co-cultured with (A) B16F10-TD-I, and (B) B16F10-TRED-I cells, corresponding to Fig. 1I, Fig. 2F. (C) CFSE labeled B16F10-TRED-I sgScramble or sg*Nlrc5* cells were co-cultured with OT-I T cells and dead B16F10-TRED-I cells were quantified by CFSE+ Zombie NIR+, corresponding to Fig. 2G.

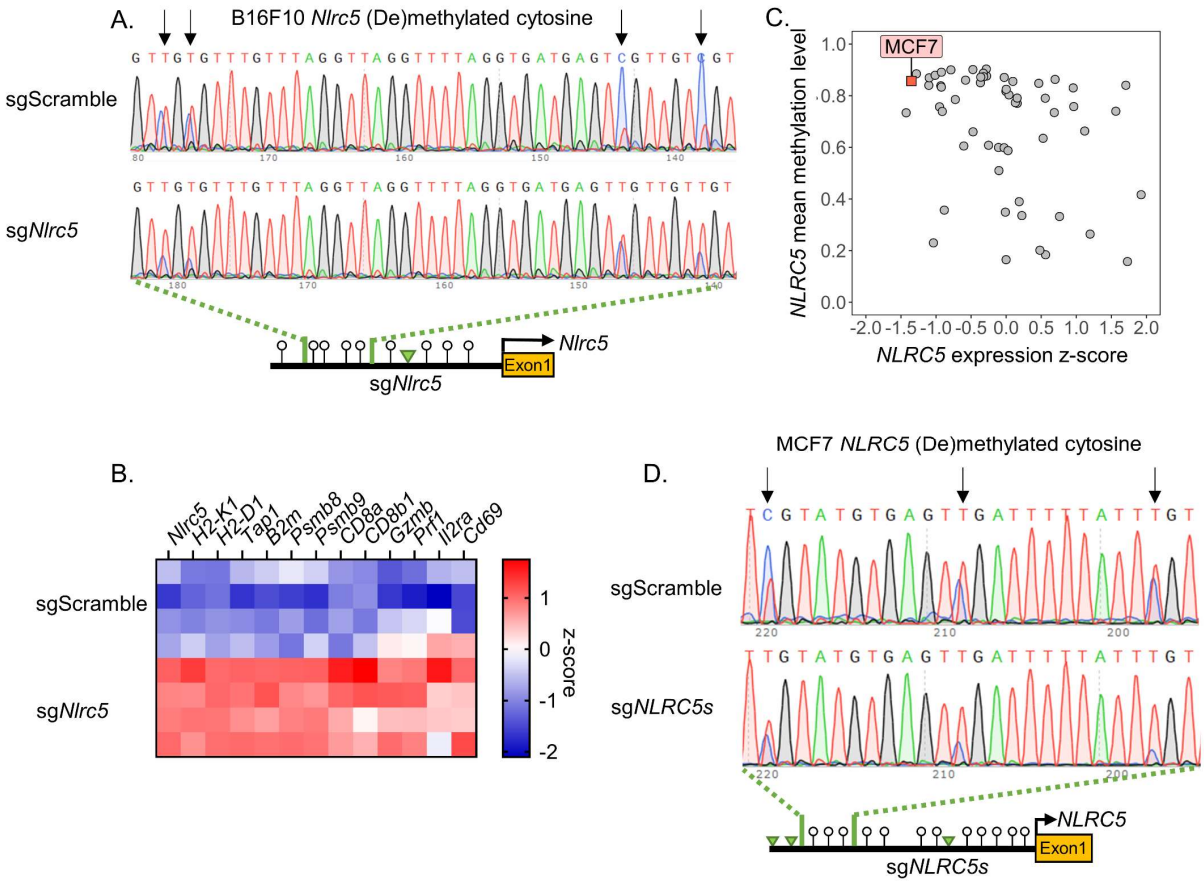

Fig. S4 The TRED-I system induced CD8+ T cell response and demethylation of *NLRC5* promoter in B16F10 and MCF7. (A) (Upper) Representative Bisulfite PCR Sanger sequencing plot quantifying the DNA methylation status of *Nlrc5* promoter in B16F10-TRED-I sgScramble and sg*Nlrc5* cells. Black arrow indicates CpG sites, corresponding to (Lower) schematic of CpG sites in *Nlrc5* promoter and Fig. 2B, Fig. S5B. (B) Heatmap plot of RNA-Seq mRNA expression levels of MHC class I antigen presentation pathway and CD8+ T cell activation and cytotoxicity markers in B16F10-TRED-I sgScramble and sg*Nlrc5* tumors. Corresponding to Fig. 3C, D. (C) Scatter plot showing the *NLRC5* methylation and expression levels of cancer cell lines from NCI60 database. *NLRC5* methylation levels are the mean from representative CpG sites in *NLRC5* promoter (cg08159663, cg16411857, and cg07839457). (D) (Upper) Representative Bisulfite PCR Sanger sequencing plot quantifying the DNA methylation status of *NLRC5* promoter in MCF7-TRED-I sgScramble and sg*NLRC5s* cells. Black arrow indicates CpG sites, corresponding to (Lower) schematic of CpG sites in *NLRC5* promoter and Fig. 6D.

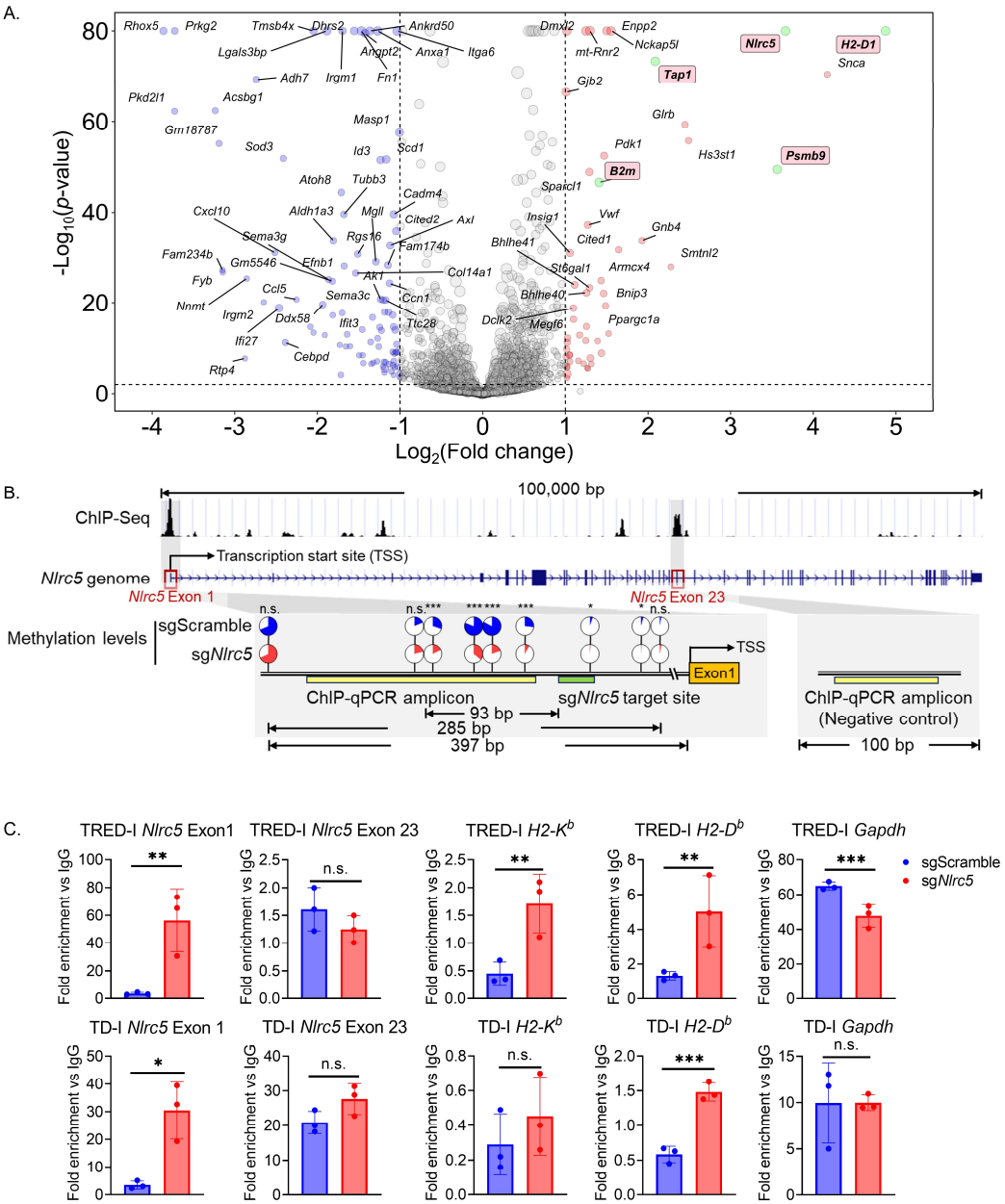

Fig. S5 Targeted demethylation of *Nlrc5* promoter specifically increased histone H3 acetylation at *Nlrc5* and MHC class I promoter. (A) Representation of major DEGs between B16F10 TRED-I sgScramble and sg*Nlrc5* cells by volcano plot, corresponding to Fig. 2D. (B) Schematic illustration of *Nlrc5* genome, its chromatin accessibility, and promoter methylation levels. (Upper) All ChIP-Seq reads for mouse tissues and cells lines (*n* = 5503) from ReMap (2022) were visualized in UNSC genome browser as peaks on *Nlrc5* genome (15, 16). Two major peaks were present adjacent to *Nlrc5* Exon 1 and 23, which were highlighted and enlarged at (Lower) depicting ChIP-qPCR amplicon, sg*Nlrc5* target site, and representation of DNA methylation levels of TRED-I sgScramble and sg*Nlrc5* cells. Location of each set of pie charts correspond to its CpG site location and colored portion indicate percentage of mean beta value with labels of statistical analysis from Fig. 2B. (C) B16F10 TD-I and TRED-I sgScramble and sg*Nlrc5* cell lysates were immunoprecipitated by anti-Histone H3 (acetyl K9 + K14 + K18 + K23 + K27) and IgG isotype control antibodies. qRT-PCR was performed on immunoprecipitated DNA using primers targeting

region adjacent to *Nlrc5* Exon 1 and 23, and promoter region of *H2-K*^{b}, *H2-D*^{b}, and *Gapdh*. CT values from each sample were normalized by its corresponding IgG control by 2^(∆Ct) method. Values shown are mean ±SD. *n* = 2 in (A), *n* = 3 in (C) for each group; '*n*' stands for number of biological replicates. Statistical significance was determined by unpaired two-sided student's *t*-test. n.s., not significant; * $p < 0.05$; ** $p < 0.01$; *** $p < 0.001$.

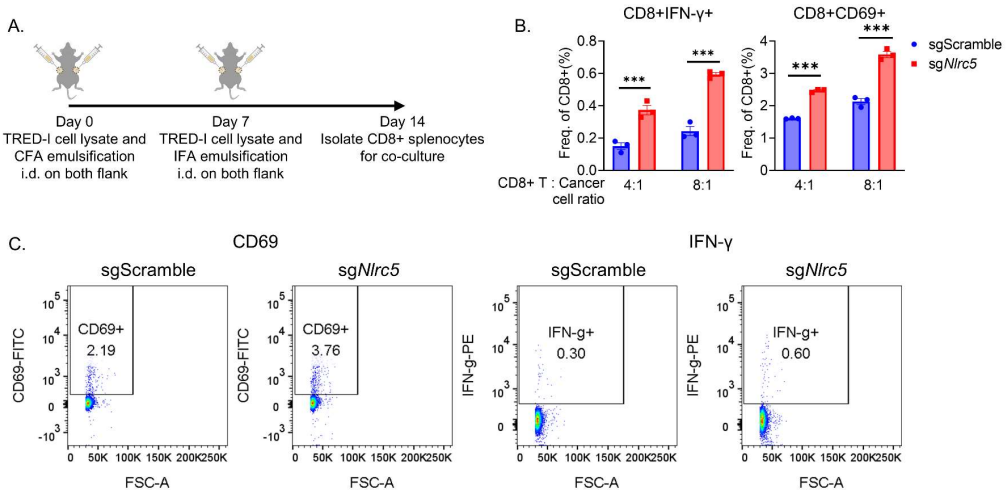

Fig. S6 Endogenous antigen presentation was increased by targeted demethylation and activation of *Nlrc5*. (A) Schematic illustration of whole tumor lysate vaccination protocol. Female C57BL/6J mice were intradermally injected on the flank with B16F10 TRED-I cell lysate-CFA emulsion on Day 0 and lysate-IFA emulsion on Day 7. (B) CD8+ T cells were isolated from spleen of whole tumor lysate vaccinated mice on Day 14 and co-cultured with TRED-I sgScramble or sg*Nlrc5* cells at CD8+ T : cancer cell ratio 4:1 and 8:1 for 24 h. Intracellular IFN-γ and surface CD69 expression levels on CD8+ T cells were quantified by flow cytometry. (C) Representative scatter plots for flow cytometry analysis from (B). Values shown are mean ±SD. n = 3 for each group in (B); 'n' stands for number of biological replicates. Statistical significance was determined by unpaired two-sided student's t-test. *** $p < 0.001$.

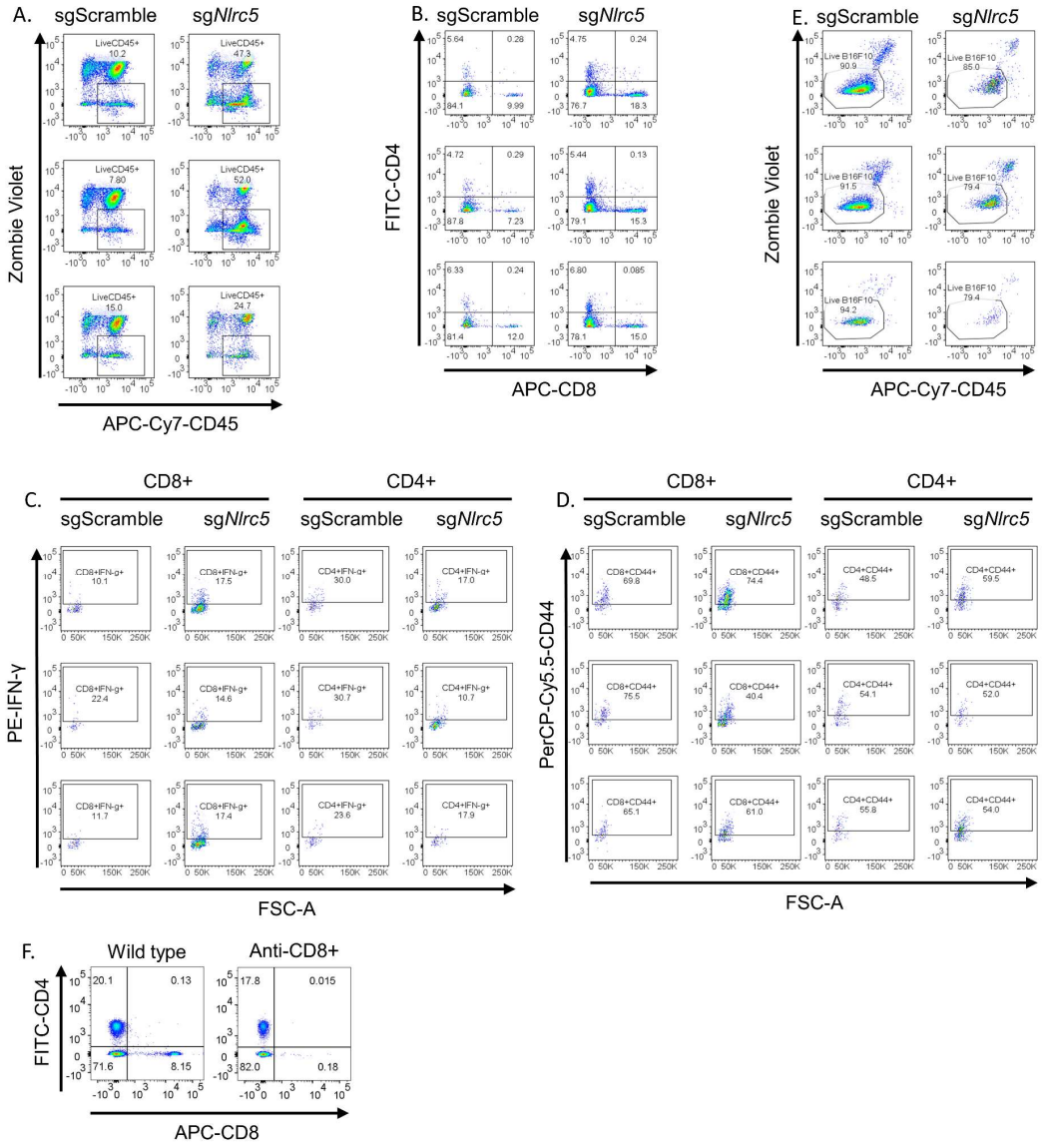

Fig. S7 Representative scatter plots for flow cytometry analysis of B16F10-TRED-I tumors and validation of CD8+ T cell depletion in C57BL/6 mice. The B16F10-TRED-I sgScramble or sg*Nlrc5* cells were implanted in C57BL/6 mice on day 0, and tumors were harvested on day 18. TILs and B16F10 cells were characterized by (A) Zombie violet– CD45+ live leucocytes, (B) CD4+ or CD8+ T cells, (C) Zombie violet– CD45– live B16F10-TRED-I cells, (D) IFN-γ+ activated CD4+ and CD8+ T cells, and (E) CD44+ effector/memory CD4+ and CD8+ T cells. Corresponding to Fig. 3E. (F) C57BL/6 mice were intraperitoneally injected with 400 μg of anti-CD8+ antibody at day –1 and day 3 before tumor implantation on day 0. Splenocytes were stained by antibodies against CD45, CD4, CD8 and analyzed by flow cytometry on day 13. Untreated wild type C57BL/6 mice were analyzed as control. Representative scatter plots of CD45+ cells were shown to confirm CD8+ T cell depletion.

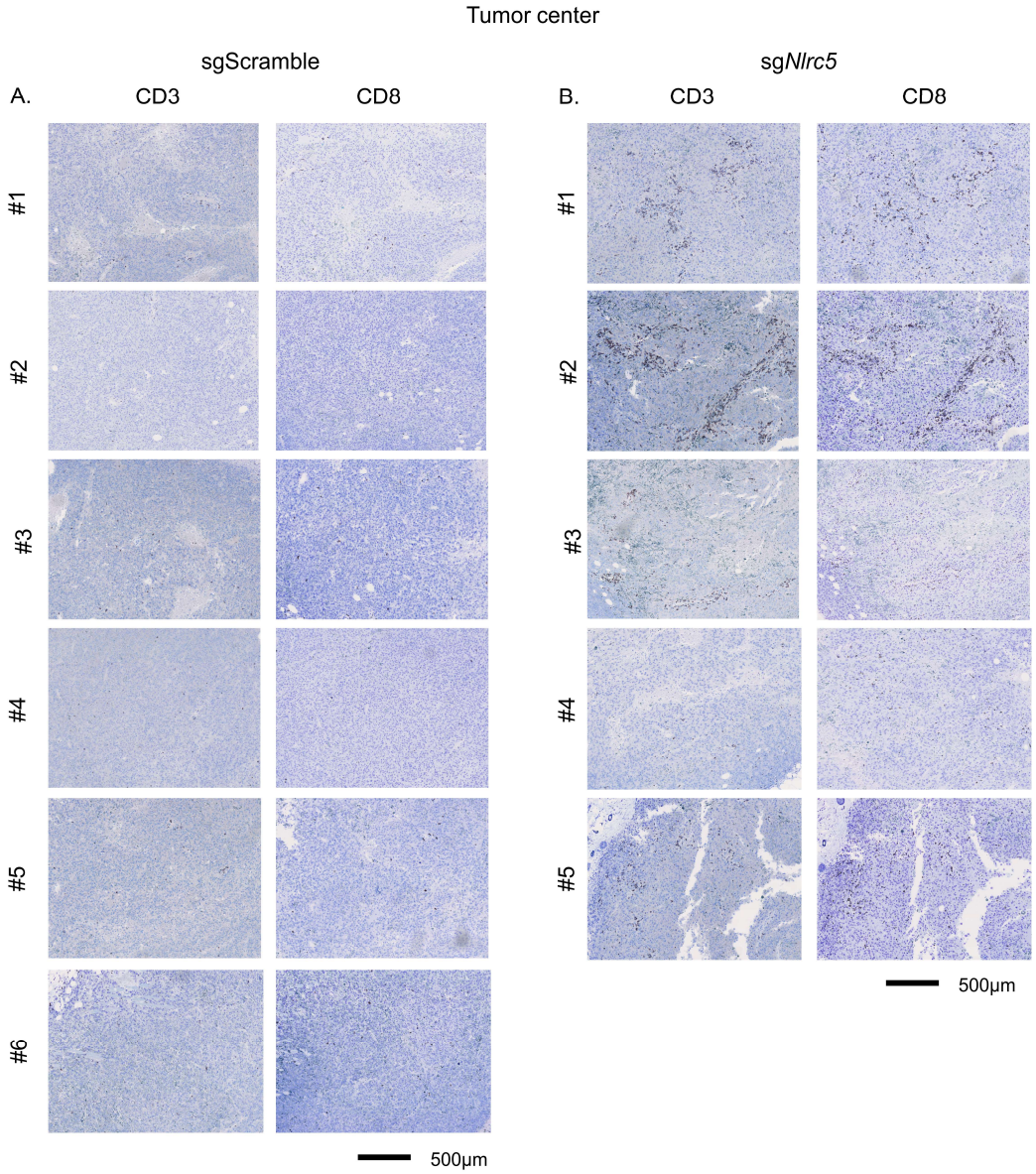

Fig. S8 Immunohistochemistry for CD3+ and CD8+ infiltrating cells in the center of sgScramble and sg*Nlrc5* tumors. B16F10-TRED-I sgScramble and sg*Nlrc5* cells were subcutaneously implanted into C57BL/6 mice on day 0 and tumors were harvested on day 18. Immunohistochemistry was performed using tumors with sufficient volume, *n* = 6 for sgScramble; *n* = 5 for sg*Nlrc5* tumors. '*n*' stands for number of mice used in the experiment. Tumor infiltrating cells were stained with anti-CD3 and -CD8 antibodies and images in the tumor center were obtained for (A) sgScramble and (B) sg*Nlrc5* tumors, corresponding to Fig. 4.

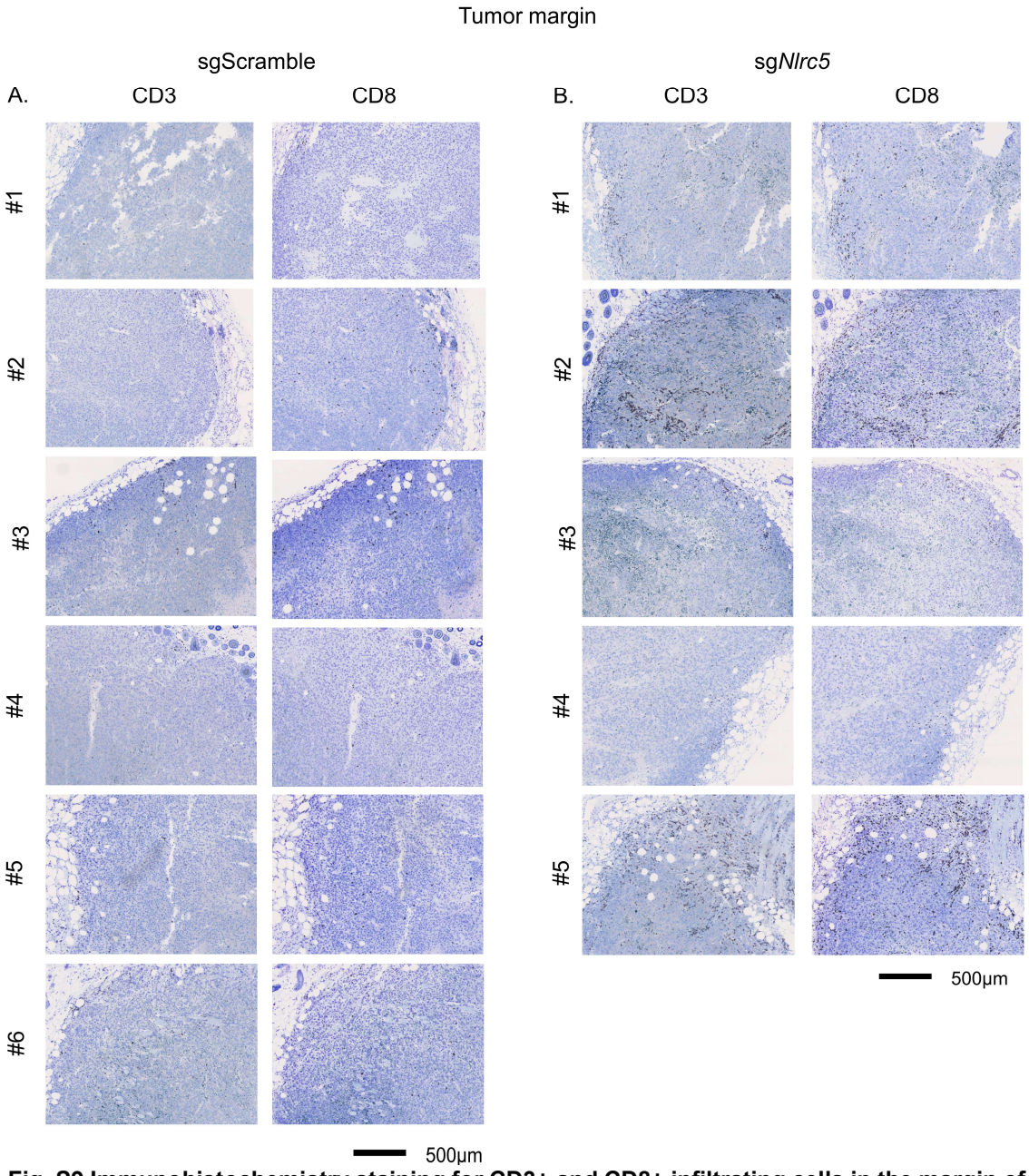

Fig. S9 Immunohistochemistry staining for CD3+ and CD8+ infiltrating cells in the margin of sgScramble and sg*Nlrc5* tumors *in vivo*. B16F10-TRED-I sgScramble and sg*Nlrc5* cells were subcutaneously implanted into C57BL/6 mice on day 0 and tumors were harvested on day 18. Immunohistochemistry was performed on tumors with sufficient volume, *n* = 6 for sgScramble; *n* = 5 for sg*Nlrc5* tumors. '*n*' stands for number of mice used in the experiment. Tumor infiltrating cells were stained with anti-CD3 and -CD8 antibodies and images in the tumor margin were obtained for (A) sgScramble and (B) sg*Nlrc5* tumors, corresponding to Fig. 4.

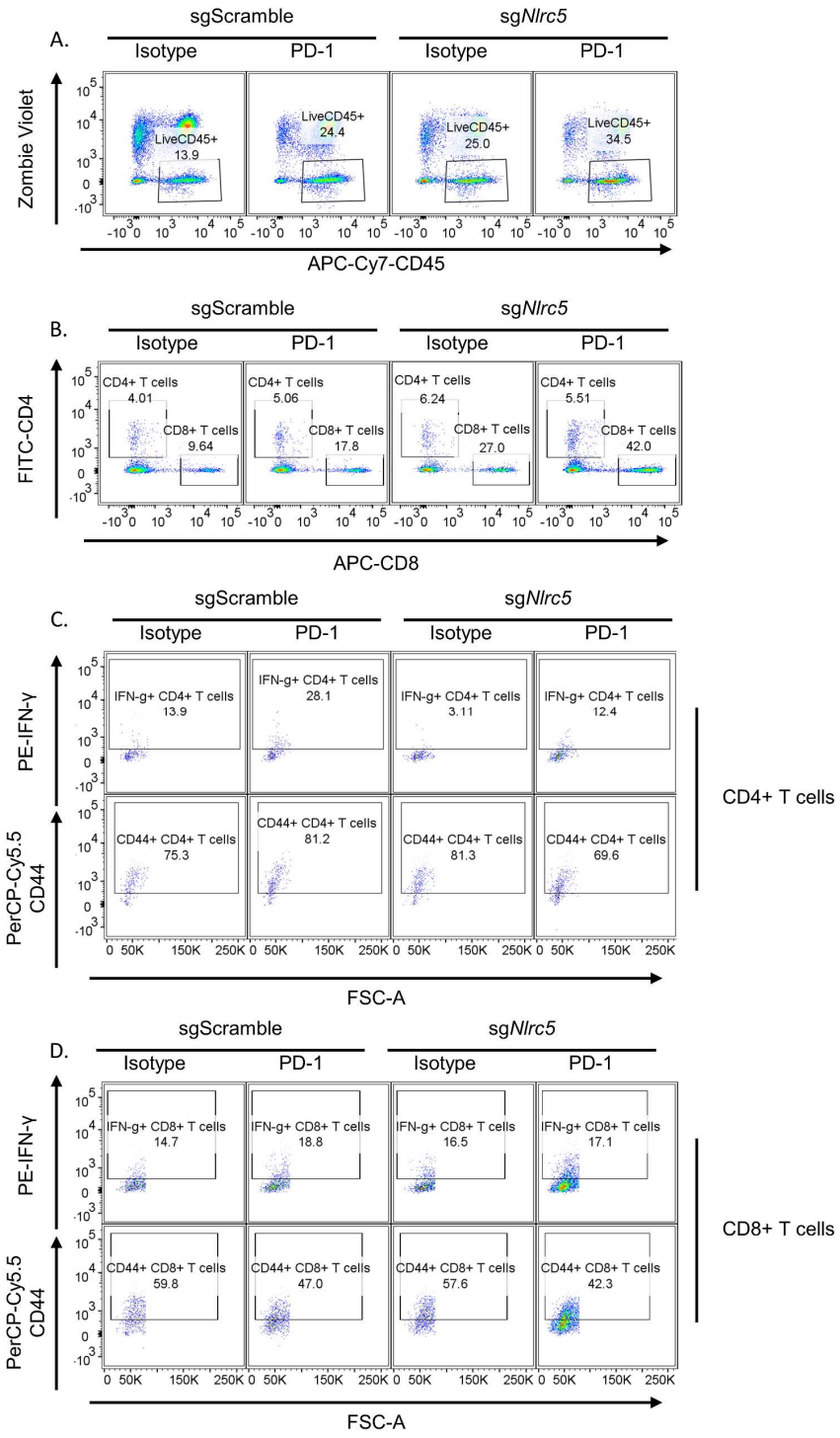

Fig. S10 Representative scatter plots for flow cytometry analysis of B16F10-TRED-I tumors implanted in C57BL/6 mice treated with isotype control or anti-PD-1 antibodies. The B16F10-TRED-I sgScramble or sg*Nlrc5* cells were implanted in C57BL/6 mice on day 0. The mice received either isotype control or anti-PD-1 antibody treatment. TRED-I-sgScramble tumors were harvested on day 15 and TRED-I-sg*Nlrc5* tumors were harvested on day 18. TILs were characterized by (A)

Zombie violet– CD45+ live leucocytes, (B) CD4+ or CD8+ T cells, (C) IFN-γ+ activated CD4+ and CD8+ T cells, and (D) CD44+ effector/memory CD4+ and CD8+ T cells. Corresponding to Fig. 5D.

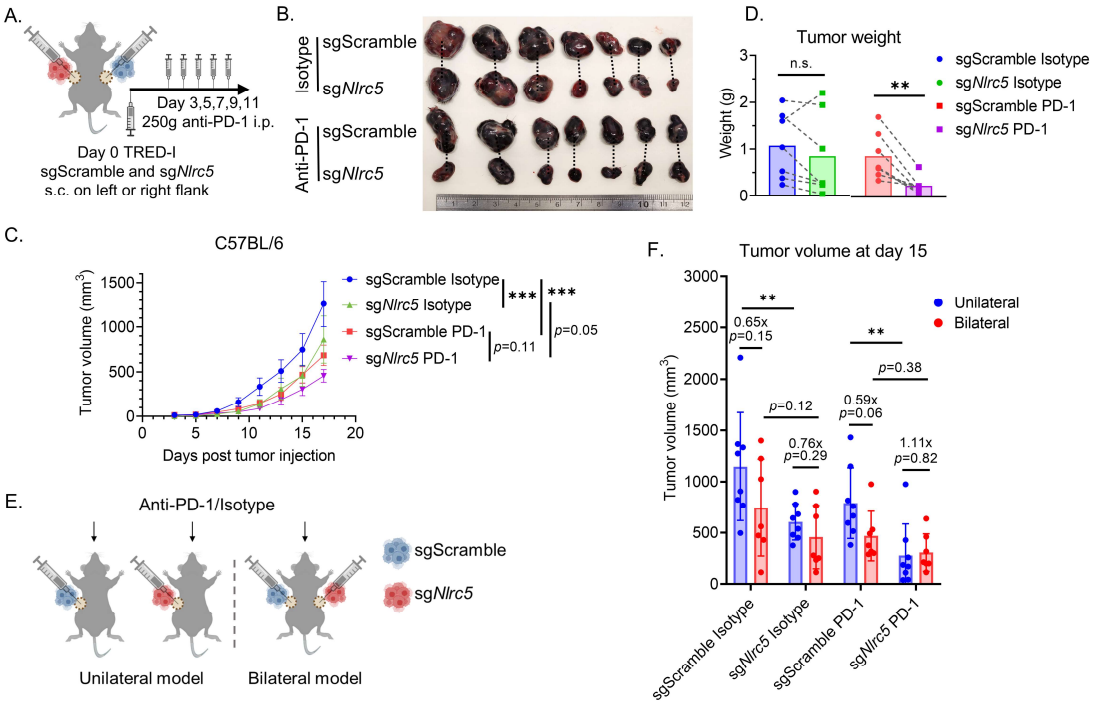

Fig. S11 Targeted demethylation and activation of *Nlrc5* may have induced anti-cancer immunity against distant tumors. (A) Schematic illustration of bilateral tumor model. On day 0, 6×10^5 of B16F10 TRED-I sgScramble or sg*Nlrc5* cells were subcutaneously injected either left or right flank of C57BL/6J mice. Anti-PD-1 or isotype antibody was intraperitoneally injected every other day from day 3 for 5 times. (B) Image of tumors harvested on day 17. Tumors connected by dashed lines were harvested from the same mouse. (C) Tumor volumes of B16F10-TRED-I sgScramble and sg*Nlrc5* tumors treated by isotype control or anti-PD-1 antibodies were estimated every other day since day 3 by digital caliper using visible tumor area and the following formula: volume (mm^3) = length * width * width / 2. (D) Tumor weight was measured and compared between TRED-I sgScramble and sg*Nlrc5* tumors harvested on day 17. Data points connected by cashed lines were the tumors harvested from the same mouse. (E) Schematic illustration of unilateral tumor model from Figure 5, and bilateral tumor model. (F) Tumor volumes on day 15 were compared between TRED-I unilateral and bilateral model with isotype or anti-PD-1 antibody treatment. Fold change of tumor volume was shown and calculated using (mean tumor volume sg*Nlrc5*) / (mean tumor volume sgScramble). Values shown in (C) are mean ±SEM and mean ±SD in (F). n = 7 in bilateral model and n = 8 in unilateral model. 'n' stands for number of biological replicates. Statistical significance was determined by two-way ANOVA test in (C), paired two-sided student's t-test in (D), and Fisher's LSD test in (F). n.s., not significant; ** $p < 0.01$; *** $p < 0.001$.

Table S1.
Oligonucleotides used in this study.

Names	Purpose	Sequence (5'-3', without NGG)
mNlrc5 #1	Mouse *Nlrc5* targeting sgRNA	GAACTTTCCAGGGCTGACGC
mNlrc5 #2	Mouse *Nlrc5* targeting sgRNA	CCTAGGCAACCCTTGCACCC
mNlrc5 #3	Mouse *Nlrc5* targeting sgRNA	CCTGGAGGCCGCGCTTGTCC
***mNlrc5* #4**	Mouse *Nlrc5* targeting sgRNA	CTTCATCCTACATCGTCTCT
mNlrc5 #5	Mouse *Nlrc5* targeting sgRNA	CTGCGATCTCCAAGCCGCGG
mNlrc5 #6	Mouse *Nlrc5* targeting sgRNA	TCAGTTTCCACAGAGCGCGG
mNlrc5 #7	Mouse *Nlrc5* targeting sgRNA	GATAGACAAACGGACTGAG
***hNLRC5* #1**	Human *NLRC5* targeting sgRNA	CACCGGATGAGTATGTCCAG
***hNLRC5* #2**	Human *NLRC5* targeting sgRNA	ATCCAACCCAGTCCCCACTG
***hNLRC5* #3**	Human *NLRC5* targeting sgRNA	TCGGACCCAAGGACAGTCCC
hNLRC5 #4	Human *NLRC5* targeting sgRNA	CAGGCATCACCCTATGTTCC
hNLRC5 #5	Human *NLRC5* targeting sgRNA	GGTGAAGGTCGGCTCACATG
hNLRC5 #6	Human *NLRC5* targeting sgRNA	CAGTTTCCCGTCCACGAAAG
BSP_*mNlrc5*_SLiCE_Fw	Cloning based bisulfite sequencing	CGGTATCGATAAGCTTGATATCTTGTATTTAGGGATTAGTAGAGAT
BSP_*mNlrc5*_SLiCE_Re	Cloning based bisulfite sequencing	CGGGCTGCAGGAATTCGATATCCATACCTCTCTAACTACTAAAACTAAAT
BSP_m*Nlrc5* _Fw	Direct bisulfite sequencing	TGTAGAATTTGGAATAGAGATAGGAATT
BSP_m*Nlrc5* _Re	Direct bisulfite sequencing	CATACCTCTCTAACTACTAAAACTAAAT
BSP_h*NLRC5*_ SLiCE_Fw	Cloning based bisulfite sequencing	ATAAGCTTGATATCGAATTCAGGTATTGAGATAGGGTTTTGG
BSP_h*NLRC5*_ SLiCE_Re	Cloning based bisulfite sequencing	CCCCCGGGCTGCAGGAATTCCTCCRCCAATACATAAAACTAA
BSP_h*NLRC5*_ Fw	Direct bisulfite sequencing	AGGTATTGAGATAGGGTTTTGG
BSP_h*NLRC5*_Re	Direct bisulfite sequencing	CTCCRCCAATACATAAAACTAA
*Nlrc5*_Fw	qRT-PCR; Mouse	CTTCCCGCCTCTCCTTCCACAAT
*Nlrc5*_Re	qRT-PCR; Mouse	CTCCACCTGCCCACATCCTACCA
H2-K^{b}_Fw	qRT-PCR; Mouse	GGCAATGAGCAGAGTTTCCGAG
H2-K^{b}_Re	qRT-PCR; Mouse	CCACTTCACAGCCAGAGATCAC
H2-D^{b}_Fw	qRT-PCR; Mouse	CCCTGTGAGCTTGGGTTCAG
H2-D^{b}_Re	qRT-PCR; Mouse	ACAGGGCAGTGCAGGGATAG
*Psmb9*_Fw	qRT-PCR; Mouse	CATGAACCGAGATGGCTCTAGT
*Psmb9*_Re	qRT-PCR; Mouse	TCATCGTAGAATTTTGGCAGCTC

*Tap1*_Fw	qRT-PCR; Mouse	GACTCCTTGCTCTCCACTCAGT
*Tap1*_Re	qRT-PCR; Mouse	AACGCTGTCACCGTTCCAGGAT
*B2m*_Fw	qRT-PCR; Mouse	ACAGTTCCACCCGCCTCACATT
*B2m*_Re	qRT-PCR; Mouse	TAGAAAGACCAGTCCTTGCTGAAG
*Ciita*_Fw	qRT-PCR; Mouse	CCCTGCGTGTGATGGATGTC
*Ciita*_Re	qRT-PCR; Mouse	ATCTCAGACTGATCCTGGCAT
*Mx1*_Fw	qRT-PCR; Mouse	CCAAAAACAAGAGACCATCAACCT
*Mx1*_Re	qRT-PCR; Mouse	CTCAGAGCCTCTGTGGTAGCAA
*NLRC5*_Fw	qRT-PCR; Human	CTGGCCAGTCTCACCGCACAA
*NLRC5*_Re	qRT-PCR; Human	CCAGGGGACAGCCATCAAAATC
*HLA-A*_Fw	qRT-PCR; Human	AAAAGGAGGGAGTTACACTCAGG
*HLA-A*_Re	qRT-PCR; Human	GCTGTGAGGGACACATCAGAG
*HLA-B*_Fw	qRT-PCR; Human	CTACCCTGCGGAGATCA
*HLA-B*_Re	qRT-PCR; Human	ACAGCCAGGCCAGCAACA
*HLA-C*_Fw	qRT-PCR; Human	GGAGACACAGAAGTACAAGCGC
*HLA-C*_Re	qRT-PCR; Human	ACATCCTCTGGAGGGTGTGAGA
*PSMB9*_Fw	qRT-PCR; Human	CGTTGTGATGGGTTCTGATTCC
*PSMB9*_Re	qRT-PCR; Human	GACAGCTTGTCAAACACTCGGTT
*TAP1*_Fw	qRT-PCR; Human	AGGGCTGGCTGGCTGCTTTGA
*TAP1*_Re	qRT-PCR; Human	ACGTGGCCCATGGTGTTGTTAT
*B2M*_Fw	qRT-PCR; Human	TGCTGTCTCCATGTTTGATGTATCT
*B2M*_Re	qRT-PCR; Human	TCTCTGCTCCCCACCTCTAAGT
*CIITA*_Fw	qRT-PCR; Human	ACAGAGCACCAAGACAGAGC
*CIITA*_Re	qRT-PCR; Human	CTCTGAGAGCTGGCACACTG
*dCas9*_Fw	qRT-PCR, Transduction validation	AACCTATGCCCACCTGTTCG
*dCas9*_Re	qRT-PCR, Transduction validation	AGGATTGTCTTGCCGGACTG
*MS2*_Fw	qRT-PCR, Transduction validation	TGGATCAGCTCCAACTCACG
*MS2*_Re	qRT-PCR, Transduction validation	TGTCTGGGTAGCCACTTTGG
*TET1*_Fw	qRT-PCR, Transduction validation	AGAAAGAAGCAGCACTCCCC
*TET1*_Re	qRT-PCR, Transduction validation	TTCGCCAAGCTGTGAAATGC
*Nlrc5*_Exon1_Fw	ChIP-qPCR, mouse	TCCCTGCACCAAGCTTTCTT

*Nlrc5*_Exon1_Re	ChIP-qPCR, mouse	CTTCGTGGAGTTGGGTCCAG
*Nlrc5*_Exon23_Fw	ChIP-qPCR, mouse	GCAGTCGAGCTAGCCTGTAG
*Nlrc5*_Exon23_Re	ChIP-qPCR, mouse	AGACCTGGCGGTCATTCTTG
H2-K^{b}_Fw	ChIP-qPCR, mouse	TCACTTCTGCACCTAACC
H2-K^{b}_Re	ChIP-qPCR, mouse	GGCTGCGTGGACTTTATATC
H2-D^{b}_Fw	ChIP-qPCR, mouse	CTTCTGCCGGGACACTGATGAC
H2-D^{b}_Re	ChIP-qPCR, mouse	GCTGATTGGCTCCTGGAATCTC
*Gapdh*_Fw	ChIP-qPCR, mouse	GAGCGGCCCGGAGTCT
*Gapdh*_Re	ChIP-qPCR, mouse	GGATTACGGGATGGGTCTGA

Supplementary references

1. Konermann S*, et al.* (2015) Genome-scale transcriptional activation by an engineered CRISPR-Cas9 complex. *Nature* 517(7536):583-588.
2. Zhang Y, Werling U, & Edelmann W (2012) SLiCE: a novel bacterial cell extract-based DNA cloning method. *Nucleic Acids Research* 40(8):e55-e55.
3. Tomayko MM & Reynolds CP (1989) Determination of subcutaneous tumor size in athymic (nude) mice. *Cancer chemotherapy and pharmacology* 24(3):148-154.
4. Schneider CA, Rasband WS, & Eliceiri KW (2012) NIH Image to ImageJ: 25 years of image analysis. *Nat Methods* 9(7):671-675.
5. Barrett T*, et al.* (2012) NCBI GEO: archive for functional genomics data sets—update. 41(D1):D991-D995.
6. Vandiver AR*, et al.* (2015) Age and sun exposure-related widespread genomic blocks of hypomethylation in nonmalignant skin. *Genome biology* 16(1):80.
7. Johnson KC, Houseman EA, King JE, & Christensen BC (2017) Normal breast tissue DNA methylation differences at regulatory elements are associated with the cancer risk factor age. *Breast Cancer Research* 19(1):81.
8. Cancer Genome Atlas N (2015) Genomic Classification of Cutaneous Melanoma. *Cell* 161(7):1681-1696.
9. Goldman MJ*, et al.* (2020) Visualizing and interpreting cancer genomics data via the Xena platform. *Nat Biotechnol* 38(6):675-678.
10. Koboldt DC*, et al.* (2012) Comprehensive molecular portraits of human breast tumours. *Nature* 490(7418):61-70.
11. Li B*, et al.* (2016) Comprehensive analyses of tumor immunity: implications for cancer immunotherapy. *Genome Biol* 17(1):174.
12. Dobin A*, et al.* (2013) STAR: ultrafast universal RNA-seq aligner. 29(1):15-21.
13. Love MI, Huber W, & Anders S (2014) Moderated estimation of fold change and dispersion for RNA-seq data with DESeq2. *Genome Biol* 15(12):550.
14. Yu G, Wang LG, Han Y, & He QY (2012) clusterProfiler: an R package for comparing biological themes among gene clusters. *OMICS* 16(5):284-287.
15. Hammal F, de Langen P, Bergon A, Lopez F, & Ballester B (2022) ReMap 2022: a database of Human, Mouse, Drosophila and Arabidopsis regulatory regions from an integrative analysis of DNA-binding sequencing experiments. *Nucleic Acids Research* 50(D1):D316-D325.
16. Kent WJ*, et al.* (2002) The human genome browser at UCSC. *Genome Res* 12(6):996-1006.

Dataset S1 (separate file). Differentially expressed gene analysis of bulk RNA-seq results.

Dataset S2 (separate file). Gene ontology (GO) analysis of bulk RNA-seq results from *in vivo* tumor.